

## Dissipative dynamic fracture of disordered systems

T.T. Rautiainen,<sup>1</sup> M.J. Alava,<sup>2</sup> and K. Kaski<sup>1</sup>

<sup>1</sup>Tampere University of Technology, Department of Electrical Engineering, P.O. Box 692, FIN-33101 Tampere, Finland

<sup>2</sup>Helsinki University of Technology, Laboratory of Physics, FIN-02150 Espoo, Finland

(Received 14 December 1994)

Breakdown of two-dimensional disordered systems is studied with a time-dependent network model. The dependence of fracture process on the local relaxation of the force field is included within the framework of Maxwellian viscoelasticity. The dynamics and characteristics of crack formation and propagation are shown to depend on disorder and relative time scales of dissipation and loading. Brittle behavior is encountered in the adiabatic limit of slow straining. At finite strain rates, the development of damage shows ductile behavior with increasing dissipation. Nucleation of cracks in various dynamical situations is discussed.

PACS number(s): 05.90.+m, 46.10.+z, 62.20.Mk, 83.50.By

The development of failure in a medium depends on defects and disorder, initially present. In such far-from-perfect systems, brittle failure has received a lot of attention due to intrinsic technological interest [1]. The strength of a material depends also on its ability to withstand damage, which is determined by the rate small scale defects grow and get connected. The final fracture occurs when a loaded specimen has a crack that has grown over a critical size. Many real materials, such as composites and polymers, display time-dependent and dissipative behavior under stress. Such materials are called *viscoelastic*, and they show creep and relaxation of applied stress [2] and stress-strain behavior that depends directly on the loading rate. The microscopic reasons for viscoelastic and reversible elastic responses differ, and in polymer melts, for example, the cause is believed to be the slow readjustment of the microscopic constituents to the applied stress. It is similar to the dynamics of dislocations, which underlies plasticity in the stress-strain characteristics of metals.

In this Rapid Communication we analyze the interplay between disorder and dissipation in dynamic fracture with a simple time-dependent mesoscale model. The beginning and development of failure have usually been studied with discrete lattice models [1,3], in which the strain is applied adiabatically. In this case the simulations are conducted in a way that corresponds to a slow rate of straining: the local stress field is allowed to readjust itself to the changes in the environment over a scale of the correlation length. Hence such quasistatic models exhibit no real dynamics, but a series of equilibrium states.

Our model is constructed to be initially a square lattice, each site being assigned a unit mass, whose dynamical behavior will be monitored. As in usual quasistatic lattice models for fracture, the sites are connected by bonds. The elastic interaction strength of a bond  $ij$  between nearest neighbor sites  $i$  and  $j$  is described by the Born Hamiltonian [4]

$$H_{ij} = \frac{\alpha}{2} [(\vec{u}_i - \vec{u}_j) \cdot \vec{d}_{\parallel}]^2 + \frac{\beta}{2} [(\vec{u}_i - \vec{u}_j) \cdot \vec{d}_{\perp}]^2, \quad (1)$$

in a system of size  $L \times L$ . The displacement vector of site  $k$  is denoted by  $\vec{u}_k$ , and  $\vec{d}_{\parallel, \perp}$  stands for the unit vector, either parallel or perpendicular to the vector connecting the sites in

the undeformed lattice. Periodic boundary conditions are applied perpendicular to the external loading, as depicted in Fig. 1. The Born potential, defining a noncentral force system, is the simplest one in describing angular stiffness, but it is computationally less demanding compared with various bond-bending Hamiltonians [5]. It also allows the study of fairly large system sizes, up to  $10^5$  particles. In our model, disorder is introduced as quenched, i.e., by removing a fraction of bonds at random with probability  $(1-p)$ .

Apart from the energetics described above, the choice for the dynamics of the system plays a crucial role in modeling fracture. This is because simultaneously a time scale is introduced. The dynamics of site-spring models has been analyzed earlier in some special cases [6], and it is closely related to discrete cellular automata and Hamiltonian systems [7]. The classical molecular dynamics simulations of fracture are also closely analogous [8,9]. Recently, some time-dependent lattice models of fracture have been devised [10–12] in which the time scale arises from stochastic rules, or is, in other words, externally dictated. In our model, a dissipation mechanism is introduced to the microscopic forces in order to mimic the local adjustment of the material structure to the stress. This is done through the classical Maxwellian viscoelasticity [13], which allows the description of relaxation and dissipation of elastic energy as a dynamical decay of the local forces. The constitutive equation for the forces acting at each bond is taken to be

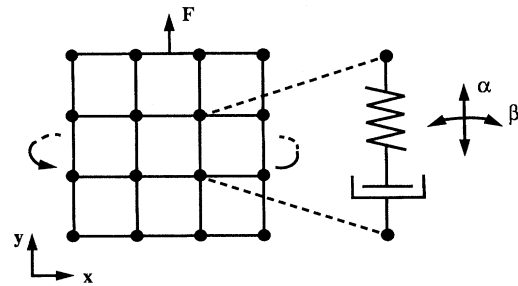


FIG. 1. Description of the model. Neighboring mass sites are coupled with dissipative Born springs, parametrized with  $\alpha$  and  $\beta$ . The dynamics of the local bond forces are given by Eq. (2). A bond exists with probability  $p$ .

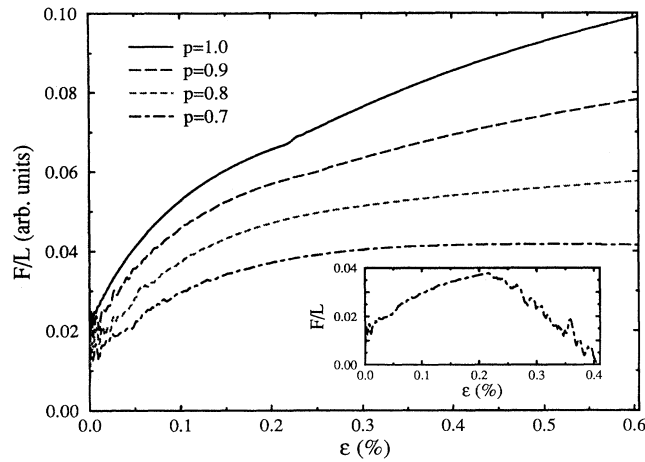


FIG. 2. Force-elongation curves for various degrees of dilution,  $p = 0.7, 0.8, 0.9$ , and  $1.0$ , with  $L = 100$  and  $\tau = 1.0$ . The inset shows the force-elongation characteristics for a single fracture simulation with  $p = 0.7$ ,  $\tau = 1.0$ , and  $L = 100$ .

$$\frac{df_{ij}}{dt} = \frac{\partial f_H}{\partial t} - \frac{1}{\tau} f_{ij}. \quad (2)$$

Here  $f_{ij}$  is the force resulting from the interaction between sites  $i$  and  $j$  and  $f_H$  is the elastic force derived from the Born Hamiltonian.  $\tau$  is a phenomenological dissipation constant, which sets the internal time scale for the relaxation of the forces. Thus our choice of local dynamics is equivalent to substitution of Maxwellian viscoelastic elements for springs obeying the Born-type linear constitutive law (see Fig. 1). For the unit mass of sites, the dissipation constant  $\tau$ , the strength of elastic interactions ( $\alpha, \beta$ ) and, under tensile loading, the average strain rate of bonds parallel to the external strain  $d\epsilon/dt$  determine the dynamic time scales of the model. In the following, if not mentioned, the strain rate is chosen to be  $d\epsilon/dt = 2.5 \times 10^{-4}$ . The Born parameters are taken as  $\alpha = 500$  and  $\beta = 250$ .

The loading characteristics, before fracture, for constantly increasing strain in our network model with  $L = 100$ , are illustrated in Fig. 2. Several force-elongation curves are shown, corresponding to increasing dilution or disorder. The general features are like those of a material displaying Maxwellian viscoelasticity. Under steadily increasing strain there is an initial region that is similar to ideal elasticity crossing over to a viscous phase, with a final state of constant force. Note that the tangent elastic modulus, or force needed for further elongation, follows the mean-field type linear density ( $p$ ) behavior observed in adiabatic models. The small oscillations in the beginning of the force-elongation curve follow from the transient in applying load to the system. With sufficient dissipation, such macroscopic oscillations decay away with increasing straining. For a small  $\tau$ , the internal stresses relax rapidly, and the system settles down to a low level of external force when strained further. For a large  $\tau$ , the system behavior resembles more and more a system of ideal Born springs. The role of the dissipation can be described through the product  $\tau d\epsilon/dt$ , which is a measure of the elastic properties of the system. Note that it also determines the

steady-state stress, which is achieved with sufficient straining. In the limit of a vanishing strain rate and dissipation, the ensuing force-elongation characteristics should be equal to those of a corresponding adiabatic model [14,15].

Next we investigate the dependence of the fracture process on the strain rate and internal dissipation via the  $\tau$  parameter. General features of fracture are shown in the inset of Fig. 2, in which a  $100 \times 100$  system is strained up to the point of failure. The initial bond dilution was chosen to be 30%, i.e.,  $p = 0.7$ , in the simulation. The calculation is stopped once the system becomes mechanically disconnected, which is checked after each bond breakage. As a fracture criterion we use the elongation of a bond: it is broken if its length exceeds a critical value, here taken as 1% of the original bond length. Note that the beginning of fracture in an “ideal” force-elongation curve is roughly given by the chosen fracture length (cf. Fig. 2). After the onset of fracture, the decrease in the force-elongation curve shows fluctuations. This is caused partly by the relaxation of the internal elastic energy contained in the lattice, and partly by disorder.

Compared to the linear dependence between local stress and strain in adiabatic models, our choice for the constitutive relation implies that the local stress depends not only on the present strain, but on the whole preceding strain history. The fracture condition in this work can be compared with that used by Sornette and Vanneste (SV), whose lattice model is based on the rupture of fuse elements, when the local temperature exceeds a critical value [12]. In that case the temperature field controlled by the individual fuse currents is analogous to the plastic strain field. However, in our model the local strain is directly responsible for the onset of fracture. In both cases, the instantaneously high stresses, or currents in the SV model, do not necessarily break the bond, but the “memory” from previous deformations—included in the bond length, or fuse temperature in the SV model—may cause the rupture at low local stress levels. In interpreting our simulations, it should also be remembered that the redistribution of internal stresses occurs with a finite speed. This is in contrast to the quasistatic models.

For a moderate to large strain rate and in a slightly diluted system, two different regimes can be seen in the fracture process. The increase in damage during the elongation can be used to demonstrate this. Figure 3 shows, for a system with  $p = 0.9$ , how the dissipation constant  $\tau$  affects the time development of the number of bonds cut during straining,  $N_c$ . For a small enough  $\tau$ ,  $\tau = 1$  at  $d\epsilon/dt = 2.5 \times 10^{-4}$ , the proportion of ruptured bonds grows rapidly in the beginning of the fracture history. But then the accumulation of damage saturates and the system is able to withstand additional straining. This can be attributed to local viscoelastic dissipation, which arrests the growth of the crack. Note that during loading, the distribution of strain in the network shows a clear bias towards the strained edge, if the strain rate is high enough. Thus, in spite of disorder, the bonds near the strained edge have a higher probability to reach the fracture condition first [16]. For a larger value of  $\tau = 10$ , one observes that the time dependence of  $N_c$  is different. After the initiation of fracture, isolated bond breakages build up slowly, until the final rupture phase, during which most of the bonds are broken in a correlated manner [17]. In Fig. 3 the latter behavior is seen as a steeper increase in  $N_c$ . This can be

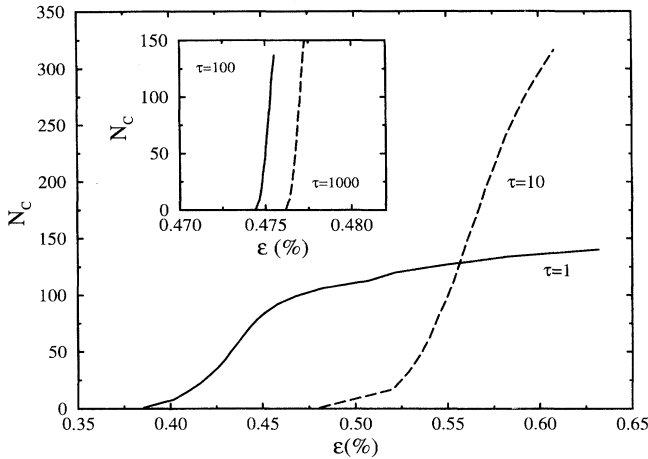


FIG. 3. Time development of the number of cut bonds  $N_c$  in  $100 \times 100$  systems with  $p=0.9$  and  $d\epsilon/dt=2.5 \times 10^{-4}$  for  $\tau=1$  and  $\tau=10$ . The inset illustrates the fracture behavior close to the adiabatic limit:  $d\epsilon/dt=2.5 \times 10^{-6}$ ,  $\tau=100$  and  $\tau=1000$ . Hence the products  $\tau d\epsilon/dt$  are equal in both the pictures. The points for the start of fracture, and thereafter the points of 5%, 10%, up to 100% of the total amount of cut bonds are averaged over several runs.

interpreted as the start of the crack propagation phase. In general, at finite strain rates and a large  $\tau$ , there can exist competing microcracks, which have nucleated from several different original defects—not only from the most critical one [18], as is common in models of brittle fracture with fixed disorder. The microcracks exhibit correlated growth and can eventually coalesce. This illustrates how fracture depends on the dynamical evolution of the individual mass sites.

Judging from the width of the fracture regime in strain or strain to final fracture (in Fig. 3), the system shows increased ductility for small  $\tau$  or non-negligible dissipation. In the limit of vanishing strain rate, the differences between the two fracture regimes described above become obscure, and the fracture dynamics become eventually identical despite a varying degree of dissipation, as shown in the inset of Fig. 3. The phenomenon of the fracture behavior being independent of the dissipation in the case without almost any inertia for very slow strain rates can be attributed to the fact that the local dissipation does not change much the *ordering* of the internal forces, which in turn dictates the local dynamics. The almost identical morphologies of the corresponding cracks shows that the adiabatic behavior of quasistatic lattice models [14,19] is encountered in this limit. We emphasize the difference between the fracture process and the load history with varying dissipation and strain rate. The former shows signs of generality stemming from the decisive role of the quenched disorder, while the latter macroscopic behavior stems from the Maxwellian viscoelastic dynamics of individual bonds.

Figure 4 shows how the individual fracture events occur in the direction perpendicular to the external strain. For the propagation speed of microcracks we have found a rough dependence  $v_{crack} \approx \sqrt{\beta}$ . In our model, there seems to be no evidence of crack bifurcation in the form exhibited by some

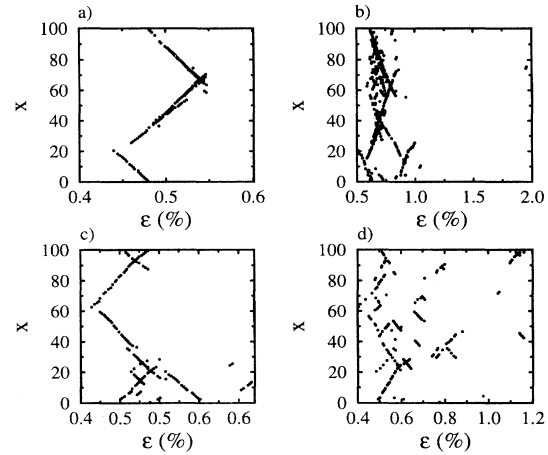


FIG. 4. The dynamical development of cut bonds perpendicular to the external strain. (a)  $\beta=250$  and  $\tau=10$ , (b)  $\beta=50$  and  $\tau=10$ , (c)  $\beta=250$  and  $\tau=1$ , (d)  $\beta=50$  and  $\tau=1$ .  $L=100$  and  $p=0.9$ , the initial dilution being identical in all cases.

recent models of crack dynamics [20], which may be caused by the differences in symmetry and loading arrangements of the system. On the other hand, it is known from studies of the quasistatic Born model in the adiabatic limit that branching and crack arrest can be controlled with the  $\alpha/\beta$  ratio [14]. This has its roots in the interactions between rows of springs parallel to the applied strain. For small values of  $\alpha/\beta$ , the fracture path becomes quite rough. However, we have chosen a moderate value in the sense that in the adiabatic case the expected cracks are rather straight in character [14]. The increased ductility for  $\tau=1$  compared with  $\tau=10$ , shown in Fig. 3, is obvious also in Figs. 4(a) and 4(c). However, decreasing  $\beta$  in Figs. 4(b) and 4(d) has a similar effect. Now it is easy for bonds to rotate to load-bearing directions, which increases the ability of the system to withstand further straining. It is also seen that the number of simultaneously propagating microcracks grows, which is attributable to the diminished interactions between the rows of bonds. Thus, concerning ductility and elastic stiffness of the systems, the  $\alpha/\beta$  ratio has a similar effect on mechanical properties as dissipation: increased ductility corresponds to a decrease in the capability of the system to store elastic energy. If the disorder is increased, i.e.,  $p$  decreases, the picture emerging from our model follows that seen in adiabatic simulations: the wandering of the final crack becomes more erratic, as the breakage of distant, individual bonds is sufficient to bring about the final fracture. The ductility and elastic modulus decrease with increasing disorder as happens in adiabatic models. The detailed study of crack statistics in the presence of branching and arrest effects is left for future study.

The main conclusion of our dissipative dynamical model is the appearance of different regimes in the fracture characteristics, when increasing the strain rate. These regimes differ in many aspects, as can be seen in the dynamics of crack growth. The most striking features are the dynamics of the final crack and the characteristics of fracture ductility. Far from the adiabatic limit, dissipation determines the ductility

of the system. Although a strongly dissipative system suffers damage at lower external strains than a weakly dissipative one, it is, however, able to accommodate more external strain, when breaking down. The differences compared to the adiabatic models arise solely from the nonlinear dissipative response of the system. This stems from the microscopic dynamics of individual sites together with the chosen fracture criterion, and is reflected in the macroscopic behavior of the system. In the opposite limit of slow dynamics, the fracture characteristics of our model approach those of standard adiabatic models. Though beyond the scope of this study, an important question arises: how do stress waves generated by individual bond breakages affect the fracture itself? It can be

expected that, in addition to disorder, the boundary conditions of the system are crucial. Finally, in judging the results, the fact should be considered that disorder in our model is assumed independent of the viscoelastic relaxation processes. This can be expected to be true in the case of physical systems with natural disorder at a mesoscopic length scale and dissipation on a molecular scale, as in such a viscoelastic material as paper. On the other hand, in polymeric materials the situation may be different.

This study was partly supported by the Technology Development Centre of Finland and the Academy of Finland. Discussions with Professor P. Duxbury are gratefully acknowledged.

- 
- [1] H.J. Herrmann and S. Roux, *Statistical Models for the Fracture of Disordered Media* (North-Holland, Amsterdam, 1990).
- [2] W. Brostow and J. Kubat, *Phys. Rev. B* **47**, 7659 (1993).
- [3] M. Sahimi, *Physica A* **186**, 160 (1992).
- [4] M. Born and K. Huang, *Dynamical Theory of Crystal Lattices* (Oxford University Press, London, 1954).
- [5] M. Sahimi and S. Arbabi, *Phys. Rev. B* **47**, 703 (1993).
- [6] P. Ossadnik, *Int. J. Mod. Phys. C* **4**, 127 (1993).
- [7] B. Chopard, *J. Phys. A* **23**, 1671 (1990).
- [8] B.K. Chakrabarti, D. Chowdhury, and D. Stauffer, *Z. Phys. B* **62**, 343 (1986).
- [9] F.F. Abraham *et al.*, *Phys. Rev. Lett.* **73**, 272 (1994).
- [10] A. Hansen, S. Roux, and E.L. Hinrichsen, *Europhys. Lett.* **13**, 517 (1990).
- [11] W.A. Curtin and H. Scher, *Phys. Rev. Lett.* **67**, 2457 (1991).
- [12] D. Sornette and C. Vanneste, *Phys. Rev. Lett.* **68**, 612 (1992);
- C. Vanneste and D. Sornette, *J. Phys. (France) I* **2**, 1621 (1992).
- [13] W. Flügge, *Viscoelasticity*, 2nd ed. (Springer-Verlag, Berlin, 1975).
- [14] G.N. Hassold and D.J. Srolovitz, *Phys. Rev. B* **39**, 9273 (1989).
- [15] J.G. Williams, *Int. J. Fract.* **33**, 47 (1987).
- [16] Note that in the case of relatively large strain rate, strong dissipation seems to affect also the rough location of the final fracture path.
- [17] The time dependence of failed bonds in simulations of brittle polymers shows similar features. See D. Blonski and W. Brostow, *J. Chem. Phys.* **95**, 2890 (1991).
- [18] P.M. Duxbury, P.D. Beale, and P.L. Leath, *Phys. Rev. Lett.* **57**, 1052 (1986).
- [19] M.J. Alava and R.K. Ritala, *J. Phys. Condens. Matter* **2**, 6093 (1990).
- [20] M. Marder and X. Liu, *Phys. Rev. Lett.* **71**, 2417 (1993).